A study of the electronic properties of ErB_2 compound by using the PBE approximation and PBE0 hybrid functional

G. Casiano Jiménez and L. Sánchez Pacheco
Grupo Avanzado de Materiales y Sistemas Complejos - GAMASCO,
Departamento de Física y Electrónica, Universidad de Córdoba, Monteria, Colombia.

J. Rodríguez Martínez
Grupo de Estudio de Materiales - GEMA, Departamento de Física,
Universidad Nacional de Colombia, Bogotá, Colombia.

D. Alejandro Rasero
Departamento de Matemática y Física, Facultad de Educación y Ciencias,
Universidad de Sucre, Sincelejo–Sucre, Colombia.
e-mail: diegorasero@gmail.com

C. Ortega López
Grupo Avanzado de Materiales y Sistemas Complejos - GAMASCO,
Departamento de Física y Electrónica, Universidad de Córdoba, Monteria, Colombia.

Received 19 November 2013; accepted 10 March 2014

We report calculations from first principles to determine the structural and electronic properties of ErB_2 compound using the Density Functional Theory (DFT) and the Full-Potential Linearized Augmented Plane Waves (FP-LAPW) method. For the description of the electron-electron interaction, the Generalized Gradient Approximation Perdew-Burke-Ernzerhof (GGA-PBE) and PBE0 Hybrid Functional were employed. From the density of states (DOS), it is found that the addition of a fraction of the exact Hartree-Fock exchange energy, in the PBE approximation, evidence the localization of the $4f$-Er orbitals, which favors electronic spin polarization of these orbitals in the ErB_2 compound. The PBE0 scheme is justified because it best describes the electronic and magnetic properties of strongly correlated systems than the PBE approximation.

Keywords: DFT; structural properties; electronic structure; diboride.

Reportamos cálculos de primeros principios para determinar las propiedades estructurales y electrónicas del compuesto ErB_2, usando la teoría del funcional densidad (DFT: Density Functional Theory) y el método ondas planas aumentadas y linealizadas en la versión del potencial completo (FP-LAPW: Full-Potential Linearized Augmented Plane Waves). Para la descripción de la interacción electrón-electrón, se emplea la aproximación del gradiente generalizado de Perdew, Burke y Ernzerhof (GGA–PBE: Generalized Gradient Approximation–Perdew-Burke-Ernzerhof) y el funcional híbrido PBE0. A partir de la densidad de estados (DOS: Density of States), se encuentra que la adición de una fracción de la energía de intercambio exacto de Hartree-Fock, en la aproximación PBE, evidencia la localización de los orbitales $4f$ del Er, lo cual favorece la polarización de los espines electrónicos de estos orbitales en el compuesto ErB_2. El esquema PBE0 se justifica porque describe mejor las propiedades electrónicas y magnéticas de los sistemas fuertemente correlacionados que la aproximación PBE.

Descriptores: DFT; propiedades estructurales; estructura electrónica; diboruro.

PACS: 71.15.Ap; 71.15.Mb; 71.15.Nc; 71.20.Eh

1. Introduction

Since the discovery of superconductivity in MgB_2 compound with AlB_2-type hexagonal crystal structure, at critical temperature $T_c \sim 40$ K [1], the research both experimental and theoretical has been intensified [2–6]. This last fact aroused a considerable interest in diboride compounds based on transition metals and rare earth elements [7–10].

The borides based on rare-earth elements have a wide variety of thermodynamic, structural, electronic and magnetic properties that make them attractive from the standpoint of science and technology. For example they are refractory, possess high hardness, high metal conductivity and high melting point [11]. Additionally borides such as tetraborides XB_4, hexaborides XB_6, and dodecaborides XB_{12}, in all cases X represents a rare earth metal, are a class of materials exhibiting various magnetic phenomena related with electronic spins of f-type orbitals [12–14]. Within this family of materials, XB_2 diborides constitute a group of compounds with AlB_2-type crystal structure, integrated by hexagonal layers composed of rare earth element atoms alternating with layers of hexagonal boron atoms [15, 16]. Experimental studies indicate that these compounds can be synthesized only at high pressures [17]. Matovnikov *et al* [18], developed a synthesis method using high pressure for a short time, followed by an annealing process with low temperatures, thus synthesized TbB_2, ErB_2, TmB_2 and LuB_2 with a 97% purity. Have been studied some properties such as heat capacity, enthalpy, entropy and Gibbs free energy [19–21], phonons [22], anoma-

lous thermal expansion, magnetic phase transitions [23–25], magnetocaloric effects [26], and isothermal sections of the phase diagram of some of these compounds [27–29].

Theoretical studies concerning to the structural and electronic properties of these materials are limited. Can be cited works based on the functional density theory (DFT) using the local density approximation (LDA) carried out for DyB_2, HoB_2, ErB_2, TmB_2, YbB_2 and LuB_2 by Fan *et al.* [8] , and for TmB_2 by Mori *et al* [24], by using pseudopotential plane waves (PP-PW) and full-potential nonorthogonal local-orbital (FPLO) methods, respectively. A recently work by Duan *et al* [30], reports DFT calculations employing PP-PW and the Generalized Gradient Approximation Perdew-Burke-Ernzerhof (GGA-PBE), for elastic constants of 24 AlB_2-type compounds, which include the diborides based on rare earth: SmB_2, GdB_2, TbB_2, ErB_2, TmB_2, YbB_2 and LuB_2.

From the theoretical point of view, as pointed Fan *et al.* [8] in their work, it should be noted that in this type of compounds, the presence of f orbitals of rare earth element implies strong electronic correlation that theoretically, is not adequately described with the local density approximation (LDA) or generalized gradient (GGA). In this case, it becomes necessary to employ exchange-correlation functionals, such as LDA + U or GGA-PBE0 [31, 32], taking into account this feature of the f orbitals.

In this work, we present a study of the electronic properties of the ErB_2 compound, using the full-potential linear method of augmented plane waves (FP-LAPW) employing exchange-correlation functionals with the LDA, GGA-PBE and GGA-PBE0 parameterizations, within the formalism of the theory of density functional. The paper is organized as follows, Sec. 2 provides a brief description of the crystal structure and the calculation conditions. In addition, there is a description of the LDA, GGA-PBE and GGA-PBE0 functionals. In Sec. 3 we show the obtained results, and finally, in Sec. 4 we present the conclusions.

2. Computational details

2.1. Crystal Structure

The ErB_2 crystallizes in AlB_2-type hexagonal crystal structure with P6/mmm (# 191) space group. In this structure, the Er atom is located within the unit cell at (0,0,0) and the B atoms at $\left(\frac{1}{3}, \frac{2}{3}, \frac{1}{2}\right)$ and $\left(\frac{2}{3}, \frac{1}{3}, \frac{1}{2}\right)$ positions.

The crystal structure shown in Fig. 1, in which B atoms are layered graphite type, with alternating layers of Er. Each Er atom has twelve B atoms as first neighbors, six in the top and six on the lower plane. To build the cell is necessary two Er layers and one of B, perpendiculars to the c axis. The distance between the B atoms is greater than the distance between the Er atoms.

2.2. Calculation Conditions

Calculations are performed within the framework of Density Functional Theory (DFT), using the Full-Potential Linearized

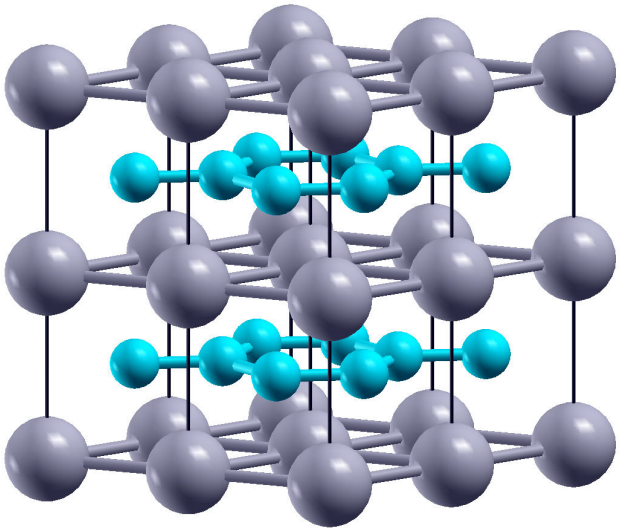

FIGURE 1. Crystal structure of the ErB_2 compound. The large spheres (in gray) represent the Er atoms and small spheres (colored cyan) atoms of B.

Augmented Plane Waves (FP-LAPW) method as implemented in the `Wien2k` software package [33]. Exchange-correlation effects are treated using the local density approximation (LDA) [34], the Generalized Gradient Approximation Perdew-Burke-Ernzerhof (GGA-PBE) [35] and PBE0 hybrid functional [31, 32].

In the LAPW method the cell is divided into two types of regions, centered atomic spheres at nuclear sites and interstitial region between the non-overlapping spheres. Within the spheres atomic, the wave functions correspond to linear combinations of products between radial and spherical harmonic functions, while in the interstitial region, the function expands as a linear combination of plane waves. The charge density and potential are expanded in spherical harmonics up to $l_{\max} = 10$, within the atomic spheres, and the wave function in the interstitial region is expanded in plane waves with cutoff parameter $K_{\max} = 8.00/r_{MT}$; where r_{MT} is the smallest radius of the atomic sphere in the unit cell and $K_{\max}$ limits the kinetic energy, $\hbar^2k^2/2m$, of plane waves with $|k| \leq K_{\max}$. To ensure convergence in the integration of the first Brillouin zone, are used 95 k-points in the irreducible part of the first Brillouin zone. The integrals over the Brillouin zone are solved using the k-point special approximation of Monkhorst-Pack [36]. The self-consistency is achieved by requiring that the convergence of the total energy is less than 10^{-4} Ry. For expanding the potential in the interstitial region is considered $G_{\max} = 12.00$. Muffin-tin radios used for Er and B were $r_{\text{MT-Er}} = 2.20$ and $r_{\text{MT-B}} = 1.60$, respectively.

2.3. LDA, GGA-PBE and PBE0 Approximations

The LDA formalism is simple and involves replacing the exchange-correlation energy at each point for an uniform

electron gas, ε_{xc}, [34]. In this approach, the exchange-correlation energy depends only of the density and is given by:

$$E_{xc} = \int \rho(\vec{r})\varepsilon_{xc}[\rho(\vec{r})]dv \quad (1)$$

In LDA the exchange–correlation effects are local, that is, dependent only of the value of the electron density at each point.

To improve the description is necessary to include the density gradient effects. In this description, referred as GGA, is taking into account the density as the density variation around each point:

$$E_{xc} = \int \rho(\vec{r})F_{xc}[\rho(\vec{r}), \nabla\rho(\vec{r})]dv \quad (2)$$

where F_{xc} is called *exchange-correlation functional*. Some of the most commonly GGA functionals used are: Perdew-Wang 86 (PW86) [37, 38], Becke-Perdew (BP) [39], Lee-Yang-Parr (LYP) [40], Perdew-Wang 91 (PW91) [41, 42], Perdew-Burke-Ernzerhof (PBE) [35], and Revised Perdew-Burke-Ernzerhof (RPBE) [43]. Most of the functionals contain a set of parameters as to replicate the energies of a serie of atoms. Among them, the PW91 functional is the only purely ab initio, as it was built using data from the uniform electron gas and exact conditions. The PBE functional corrects some defects of the PW91 functional, but the resulting energies are practically the same. The RPBE functional modifies the exchange local part of PBE functional. The LDA and PBE functional provide incorrect descriptions in compounds possessing d and f localized electrons, for example, in transition metals and rare earth elements, respectively [24, 44]. The hybrid functionals contain a fraction of Hartree-Fock exchange. Becke [45] showed that the expression

$$E_{xc} = \int_0^1 d\lambda E_{xc,\lambda}, \quad (3)$$

where λ is an interelectronic parameter with a strong coupling, allows building correlation-exchange functional approximations. The first approach was a linear interpolation

$$E_{xc}^{hyb} = \frac{1}{2}\left(E_x + E_{xc,\lambda=1}^{DFT}\right) \quad (4)$$

where E_x the exchange energy of the non-interacting system and the second term is the exchange-correlation energy of the interacting real system. After a third parameter was included for the hybrid functional [46]. Subsequently, Becke [47] proposed that a single coefficient was sufficient to determine the contribution of Hartree-Fock to DFT exchange

$$E_{xc}^{hyb} = E_{xc}^{DFT} + a_0\left(E_x - E_x^{DFT}\right) \quad (5)$$

Perdew *et al.* [48] showed that the optimum value of the coefficient must be taken as $1/4$.

The PBE0 hybrid functional [31, 32] uses the PBE-GGA for E_{xc}^{DFT}. Novak *et al.* [44, 49] proposed an improvement to describe strongly correlated electrons by subtracting the LDA or GGA exchange energy functional corresponding to the subspace of the states of the correlated electrons and to add the Hartree-Fock expression. This method called *exact exchange* for correlated electrons was implemented in the `Wien2k` code. Tran *et al.* [50] constructed an exchange-correlation energy functional of the PBE0 hybrid form

$$E_{xc}^{PBE0} = E_{xc}^{PBE}[\rho] + \frac{1}{4}\left(E_x^{HF}[\psi_{sel}] - E_x^{PBE}[\rho_{sel}]\right) \quad (6)$$

where ψ_{sel} and ρ_{sel} are, the wave function and the corresponding electronic density for selected electrons, respectively. In this functional a fraction of HF exchange replaces the PBE-GGA exchange for selected electrons. Electronic correlation is represented by the part of the PBE correlation.

In this work, we used LDA, PBE-GGA and the hybrid PBE0 functionals for ErB_2 compound. We have selected the $4f$ electrons of Er to build $E_x^{HF}[\psi_{sel}]$ and $E_x^{PBE}[\rho_{sel}]$ indicated in the Eq. (6).

TABLE I. Lattice parameters calculated in this work, theoretical values of other authors and experimental values reported for ErB_2. Lattice parameters are reported of the structure at equilibrium (a, c/a), the minimum volume V_0, the bulk modulus B_0, the minimum energy E_0, and the magnetic moment per cell μ.

Reference	Method	a (Å)	c/a	V_0 (Å)	B_0 (GPa)	E_0(eV)	μ (μ_0/cell)
This work	FP-LAPW: LDA	3.168	1.191	32.78	168.81	-11.085	2.66
This work	FP-LAPW: GGA-PBE	3.247	1.182	35.02	148.71	-14.896	2.70
This work	FP-LAPW: GGA-PBE0	3.260	1.166	34.98	168.33	-13.713	3.07
[8]	PP-PW: LDA	3.28	1.155	–	–	–	–
[30]	PP-PW: GGA	3.268	1.158	–	–	–	–
[18]	Experimental	3.268	1.157	–	–	–	–
[22]	Experimental	3.268	1.157	–	–	–	–
[29]	Experimental	3.265	1.155	–	–	–	–
[52]	Experimental	3.271	1.156	–	–	–	–

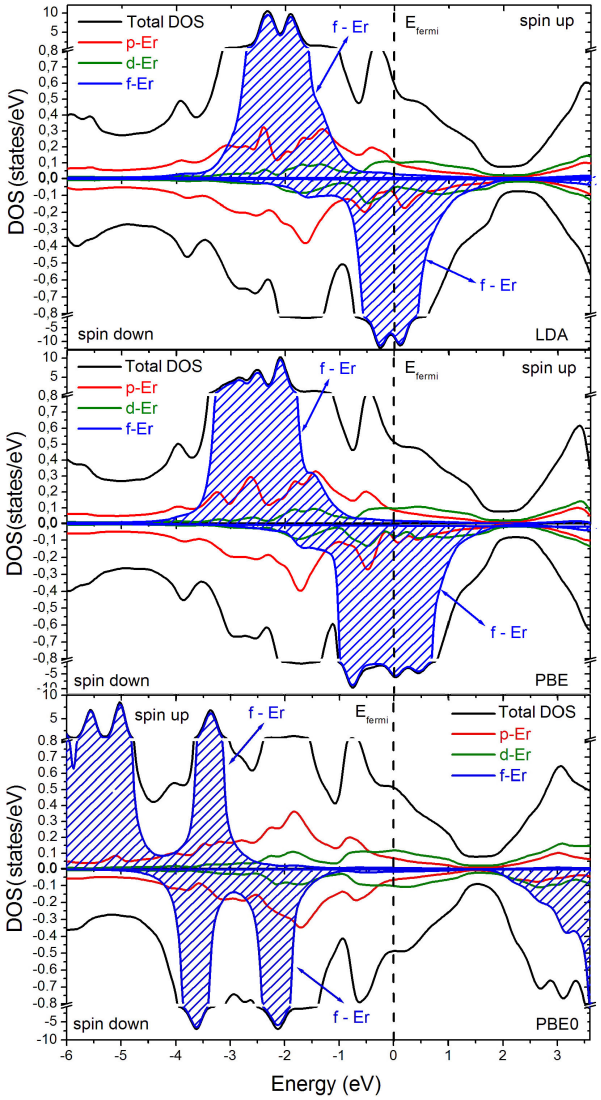

FIGURE 2. Total and partial density of states for ErB_2 with the LDA parameterization (top), GGA-PBE (middle) and GGAG-PBE0 (bottom). Are shown the contributions of the p-B, d-and f-Er states with red, green and blue shaded area, respectively. The black color line represents the total density of states. The zero of the energy is taken as the Fermi level.

3. Results and discussions

3.1. Structural Properties

To determine the structural parameters, the total energy is computed for different values of cell volume. The lattice parameters of the crystal structure, at equilibrium, are obtained by minimizing the energy as a function of volume. To perform this, we fit the obtained energy, by the equation of state of Murnaghan [51]. From this fit, we get the lattice parameter a, the ratio c/a, the minimum volume V_0, the bulk modulus B_0 and the minimum energy E_0.

The calculated values in this work, the theoretical values reported by other authors and some available experimental values are shown in Table I.

The difference between our value of the lattice parameter a and other theoretical reports does not exceed 3.5 % for the LDA calculation [8]. The difference from the theoretical value GGA [30] is of the order of 1 %.

With respect to the experimental values, the difference of our LDA and GGA values is less than 3.2 %. The GGA-PBE0 value obtained in this work differs around 0.3 % compared to the experimental values.

Additionally, LDA calculation of the ratio c/a differing by less than 3.2 % compared to the theoretical value reported by Fan *et al.* [8]. The GGA-PBE result is less than 2.1 %, compared with the value of Duan *et al.* [30]. By comparison, with respect to the experimental values, the difference in the GGA and LDA calculations does not exceed $\sim$ 3%. Our GGA-PBE0 value differs about 1 % of the experimental value.

B_0 values are obtained for the range of values corresponding to the monocrystalline silicon (130-160 GPa) and AISI 304 stainless steel (187-200 GPa) [53], indicating the ErB_2 is a relatively rigid material. This property, due to the strong bonds that exist between boron atoms present in the AlB_2-type hexagonal structure, makes it attractive for potential applications in devices operating at high temperatures.

3.2. Electronic Properties: Density of states (DOS)

The total (DOS) and partial (PDOS) density of states calculated for ErB_2 are shown in Fig. 2. The calculations were carried out considering spin polarization (DOS calculated with spin up and down polarization). In this figure we consider only the orbitals that have the greatest contribution to the Fermi level. It is observed that in all three cases the compound exhibits metallic behavior, due to the presence of half full atomic orbitals crossing the Fermi level.

From the qualitative point of view, the LDA and GGA-PBE parameterizations produce similar results for the spin up polarization, the largest contribution to the Fermi level is mainly due to p-B and d-Er states, while f-Er states are located between energy $\sim$ -3.5 eV and $\sim$ -1.0 eV. For spin down polarization, the largest contribution at the Fermi level is due to f-Er states in the energy region $\sim$ -1.5 eV and $\sim$ 0 eV.

This result explains why the LDA and GGA-PBE magnetic moment values, in Table I, are quite close (difference of 0.04 μ_0/cell). For the GGA-PBE0 calculations we found notable differences with respect to LDA and GGA-PBE. The density of electronic states GGA-PBE0 shows the f-Er localized states before the Fermi level in the region from $\sim$ -6.0 eV to $\sim$ -2.5 eV for spin up polarization, and between $\sim$ -4.0 eV to $\sim$ -1.5 eV for spin down polarization. Is not observed a significant mixing with other states of the valence band outside this region. Thus, f-Er states, particularly the $4f$ are highly localized and can only interact via a RKKY (Ruderman-Kittel-Kasuya-Yosida) interaction as noted by Mori *et al.* [24] on a theoretical and experimental study of ferromagnetism and electronic structure of TmB_2.

In the region -4 eV $< E < E_{\text{Fermi}}$ there are contributions from $2p$ states of B and $5d$ of Er. The latter, crossing the Fermi level and are responsible for the metallic character of the material. This feature distinguishes the calculated DOS with GGA-PBE0 those obtained from LDA and GGA-PBE in which f-Er states with spin down polarization cross the Fermi level.

For the energy values of $\sim$ -1.0 eV and $\sim$ -2.0 eV two peaks are observed that are characteristic of the diboride compounds based on rare-earth elements. This behavior is consistent with the results of Mori *at al*. [24] for TmB_2 and YbB_2.

It can be noted, moreover, that the differences between the derived DOS from the LDA, GGA- PBE and GGA-PBE0 parameterizations, must be, as explained Nourmohammadi *et al*. [44], in which the exchange splitting using PBE0 increases, causing that the localization of magnetic electrons (mainly the $4f$ of Er) is greater, and that the values of the lattice constant at equilibrium, and magnetic moment predicted by GGA-PBE0 be slightly greater than the results of GGA-PBE and LDA as shown in Table I.

4. Conclusions

Were determined structural and electronic properties of the ErB_2 compound, using the linearized augmented plane wave scheme in the version of the full potential and density functional theory. It was found that the effect of adding a fraction of the exact exchange energy of Hartree-Fock in PBE approximation, evidence the localization of $4f$ orbitals of Er, which favors electronic spin polarization of these orbitals in the ErB_2 compound. This explains the increase in the total magnetic moment PBE0 (3.07 μ_0/cell) compared to the total magnetic moment in PBE (2.70 μ_0/cell).

Acknowledgements

We want to thank to Universidad de Córdoba, Colombia, for the financial support during the carrying out of this study.

1. J. Nagamatsu, N. Nakagawa, T. Muranaka, Y. Zenitani and J. Akimitsu, *Nature* **410** (2001) 63.
2. R. Nuñez and A. Reyes, *Rev. Mex. Fis.* **48** (2001) 391.
3. S. Segura, R. Baquero and J. A. Rodríguez, *Rev. Col. Fis.* **36**(3) (2006) 1162.
4. J. M. An and W. E. Pickett, *Phys. Rev. Lett.* **86** (2001) 4366.
5. K.D. Belashchenko, M. van Schilfgaarde and V. P. Antropov, *Phys. Rev. B* **64** (2001) 092503.
6. P. P. Singh, *Phys. Rev. Lett.* **87** (2001) 087004.
7. P. de la Mora, M. Castro and G. Tavizon, *Journal of Solid State Chemistry* **169** (2002) 168.
8. Y. Fan, H. Ru-Shan, T. Ning-Hua and G. Wei, *Chin. Phys. Lett.* **19**(9) (2002) 1336.
9. A. K. M. A. Islam, A. S. Sikder and F. N. Islam, *Physics Letters A* **350** (2006) 288.
10. N. Hamdad, N. Benosman and B. Bouhafs, *Physica B* **405** (2010) 540.
11. K. E. Spear, *Phase Behaviour and Related Properties of Rare-Earth Borides, Phase Diagrams, Materials Science, and Technology*, vol. 4: *The Use of Phase Diagrams in Technical Materials*, Alper, A. M., Ed., 1976, pp. 91-159.
12. K. H. J. Buschow, *Boron and Refractory Borides* (Berlin, Heidelberg, 1977) p. 494.
13. D. Gignoux, D. Schmitt, *Handbook of Magnetic Materials*, edited by K. H. J. Buschow (North-Holland, Amsterdam, 1997), Vol. 10, p. 239.
14. T. Mori, Higher Borides, in *Handbook on the Physics and Chemistry of Rare-earths*, edited by K. A. Gschneidner, Jr., J.-C. Bunzli, and V. Pecharsky (North-Holland, Amsterdam, 2008), Vol. 38, p. 105.
15. G. V. Samsonov and T. I. Serebryakova, *Borides*, (Atomizdat, Moscow, 1975).
16. *Handbook of High-Melting Compounds: Properties, Production, and Applications*, (Ed. by T. Ya. Kosolapova, Metallurgiya, Moscow, 1986; Hemisphere, New York, 1990).
17. J. Cannon, M. Cannon and H. Hall, *Journal of the Less-Common Metals* **56**(1) (1997) 83.
18. A. Matovnikov, V. Urbanivich, T. Chukina, A. Sidorov, V. Novikov, *Inorganic Materials* **45**(4) (2009) 366.
19. V. Novikov and A. Matovnikov, *Russian Journal of Physical Chemistry A* **481**(4) (2007) 659.
20. V. Novikov and A. Matovnikov, *Journal of Thermal Analysis and Calorimetry* **88**(42) (2007) 597.
21. M. Avila, S. Bud'ko, C. Petrovic, R. Ribeiro, P. Canfield, A. Tsvyashchenko and L. Fomicheva, *Journal of Alloys and Compounds* **358** (2003) 56.
22. V. Novikov, T. Chukina, A. Verevkin, *Physics of the Solid State*, **52**(2) (2010) 364.
23. V. Novikovand A. Matovnikov, *Inorganic Materials*, **44** (2008) 134.
24. T. Mori, T. Takimoto, A. Leithe-Jasper, R. Cardoso-Gil, W. Schnelle, G. Auffermann, H. Rosne and Y. Grin, *Physical Review B*, **79**(10) (2009) 104418.
25. N. Novikov, A. Matovnikov, D. Avdashchenko, B. Kornev, V. Solomennik, V. Novikova and O. Marakhina, *Physics of the Solid State*, **52**(1) (2010) 142.
26. Z. Han, D. Li, H. Meng, X. Liu and Z. Zhang, *Journal of Alloys and Compounds*, **498** (2010) 118.
27. N. Chaban, S. Mikhalenko, Y. Kernitska and Y. Kuz'ma, *Powder Metallurgy and Metal Ceramics*, **40**(5-6) (2011) 258.

28. I. Veremchuk, N. Chaban, V. Davydov and Y. Kuz'ma, *Inorganic Materials*, **40**(12) (2004) 1301.
29. J. Roger, V. Babizhetskyy, T. Guizouarn, K. Hiebl, R. Guérin and J. Halet, *Journal of Alloys and Compounds* **417** (2006) 72.
30. Y. H. Duan, Y. Sun, Z. Z. Guo, M. J. Peng, P. X. Zhu and J. H. He, *Computational Materials Science* **51** (2012) 112.
31. M. Ernzerhof, G. E. Scuseria, *J. Chem. Phys.* **110** (1999) 5029.
32. C. Adamo, V. Barone, *J. Chem. Phys.* **110** (1999) 6158.
33. P. Blaha, K. Schwarz, G. Madsen, D. Kvasnicka and J. Luitz. `WIEN2k`, *An Augmented Plane Wave Plus Local Orbitals Program for Calculating Crystal Properties* (Vienna University of Technology) 2009. ISBN 3-9501031-1-2
34. P. Hohenberg, W. Kohn, *Phys. Rev.* **136** (1964) B864.
35. J. P. Perdew, K. Burke and M. Ernzerhof, *Phys. Rev. Lett.* **77** (1996) 3865.
36. H. J. Monkhorst, A. T. Pack, *Phys. Rev. B* **13** (1976) 5188.
37. J. P. Perdew, *Phys. Rev. B* **33** (1986) 8822.
38. J. P. Perdew, Y. Wang, *Phys. Rev. B* **33** (1986) 8800.
39. A. Becke, *Phys. Rev. A* **38** (1988) 3098.
40. C. Lee, W. Yang, R. G. Parr, *Phys. Rev. B* **37** (1988) 785.
41. J. P. Perdew, J. A. Chevary, S. H. Vosko, K. A. Jackson, M. R. Pederson, D. J. Singh, C. Fiolhais, *Phys. Rev. B* **46** (1992) 6671.
42. J. P. Perdew, Y. Wang, *Phys. Rev. B* **45** (1992) 13244.
43. B. Hammer, L. B. Hansen, J. K. Nørskov, *Phys Rev. B* **59** (1999) 7413.
44. A. Nourmohammadi, M. R. Abolhasani, *Solid State Communications* **150** (2010) 1501.
45. A. D. Becke, *J. Chem. Phys.* **98** (1993) 1372.
46. A. D. Becke, *J. Chem. Phys.* **98** (1993) 5648.
47. A. D. Becke, *J. Chem. Phys.* **104** (1996) 1040.
48. J. P. Perdew, M. Ernzerhof, K. Burke, *J. Chem. Phys.* **105** (1996) 9982.
49. P. Novák, J. Kunes, L. Chaput, W. E. Pickett, *Phys. Status Solidi B*, **243** (2006) 563.
50. F. Tran, P. Blaha, K. Schwarz, P. Novák, *Phys. Rev. B* **74** (2006) 155108.
51. F. Murnaghan, *Proceedings of the National Academy of Sciences* **30**(9) (1944) 244.
52. P. Vallars, *Pearson's Handbook: Crystallographic Data for Intermetallic Phases*, (ASM International, Materials Park, OH, 1997).
53. J. M. Meza, E. E. Franco, M. C. M. Farias, F. Buiochi, R. M. Souza and J. Cruz, *Revista de Metalurgía* **44**(1) (2008) 52.